

Photoacoustic Measurements of Thermal Conductivity at Elevated Temperatures

Changrui Cheng and Xianfan Xu^{*}
School of Mechanical Engineering
Purdue University

Abstract

This work describes applying the photoacoustic (PA) technique to the measurement of thermal conductivity at elevated temperatures. The PA technique has been shown to be successful for thermal conductivity measurements at the room temperature, yet no measurements have been performed at high temperatures. In this work, the design of photoacoustic cell for high temperature measurement is described in detail. The maximum measurement temperature is limited by the operation temperature of the microphone and its accessories used in this work. Measurement results of a ceramic sample will be discussed. The photoacoustic theory for measuring thermal properties of a sample with an arbitrary number of thin film layers and contact resistances will also be described.

Keywords: thermal conductivity, photoacoustic method, high temperature

I. Introduction

Thermal conductivity is one of the most important properties for understanding and calculating the heat transfer process in a material [1]. Many techniques have been developed to measure thermal conductivity of materials, which can be characterized into contact and non-contact methods. The contact methods, such as using thermocouples or thin film thermistors, introduce errors caused by contact resistances, and are often time consuming in preparation of experiments [2]. On the other hand, the non-contact techniques, such as optical techniques, are generally more flexible in terms of the types of materials can be measured and require minimum sample preparation.

The photoacoustic (PA) technique is a non-contact method that has been used successfully to measure thermal conductivity of many materials [2, 3]. As first explained by Rosencwaig and Gersho [4], the PA signal is the result of thermal expansion of the gas adjacent to the sample surface that is heated by some modulated thermal sources. Since then, the PA technique has been investigated by many researchers to expand its capability [2, 3, 5, 6]. The principle of the PA method can be explained as follows. A heating source (for example, a laser beam) with periodic heating pulses is applied on the sample surface. Thus, the temperature of the air above the sample changes periodically due to conduction from the sample, and an acoustic wave is generated because of the thermal expansion of the air. This acoustic wave is sensed by the microphone, and its amplitude can be related to thermal properties of the sample. Therefore, by analyzing the magnitude and/or phase of the acoustic wave, thermal conductivity of the sample is obtained.

^{*} To whom correspondence should be addressed. Phone: (765) 494-5639, Fax: (765) 494-0539, Email: xxu@ecn.purdue.edu

Our previous work was focused on PA measurements at the room temperature [2, 3]. However, for many situations, values of thermal conductivity at higher temperatures are needed. In this work, we describe development of an experimental apparatus for high temperature measurements. The design of the photoacoustic cell capable of measuring thermal conductivity at elevated temperatures is described in detail. Preliminary experimental results on a ceramic sample are presented.

II. Photoacoustic Theory

A PA theory has been developed to handle measurements of multiple layer samples with contact resistance between any two adjacent layers [2, 3]. The mathematic formulation is briefly described here. The sample is assumed to have a backing material (0) and N successive layers. A certain type of gas, such as the air, is above the sample as the N+1 layer. The top surface is heated by a modulated laser beam, whose intensity is of the form of $0.5I_0(1+\cos(\omega t))$, where I_0 is the maximum incident laser intensity and ω is the angular modulation frequency of the laser beam. It is shown that if the dimension of the photoacoustic cell is much larger than the thermal diffusion length in the gas, the photoacoustic signal (the pressure signal in the gas) is independent of the lateral laser energy distribution on the sample surface, and the PA effect can be described using a 1-D formulation. Treating the absorbed laser power in each layer as the internal energy source and applying interface boundary conditions of temperature and heat flux continuity, the 1-D heat conduction equation can be solved analytically to obtain the transient temperature in each layer and in air. The detailed derivation process is described elsewhere [2, 3]. The resulting complex temperature distribution in the air (layer number N+1) can be written as:

$$q_{N+1} = (1 - r) B_{N+1} e^{-s_{N+1}x} e^{j\omega t}, \quad (1a)$$

where r is the reflectivity of the sample surface, and x is the coordinate along the thickness direction. $s_i = T_i - T_0$ is the modified temperature in layer i , and T_0 is the ambient temperature. The expression for B_{N+1} is

$$B_{N+1} = - \frac{[0 \quad 1] \sum_{m=0}^N \left\{ \left(\prod_{i=0}^{m-1} U_i \right) V_m \begin{bmatrix} E_m \\ E_{m+1} \end{bmatrix} \right\}}{[0 \quad 1] \left(\prod_{i=0}^N U_i \right) \begin{bmatrix} 0 \\ 1 \end{bmatrix}} \quad (1b)$$

and

$$U_i = \frac{1}{2} \begin{bmatrix} u_{11,i} & u_{12,i} \\ u_{21,i} & u_{22,i} \end{bmatrix}; \quad V_m = \frac{1}{2} \begin{bmatrix} v_{11,m} & v_{12,m} \\ v_{21,m} & v_{22,m} \end{bmatrix}; \quad (1c)$$

$$u_{1n,i} = (1 \pm k_{i+1} s_{i+1} / k_i s_i \mp k_{i+1} s_{i+1} R_{i,i+1}) \exp(\mp s_{i+1} l_{i+1}), \quad n = 1, 2; \quad (1d)$$

$$u_{2n,i} = (1 \mp k_{i+1} s_{i+1} / k_i s_i \mp k_{i+1} s_{i+1} R_{i,i+1}) \exp(\mp s_{i+1} l_{i+1}), \quad n = 1, 2; \quad (1e)$$

$$v_{n1,m} = 1 \pm b_m / s_m, \quad n = 1, 2; \quad (1f)$$

$$v_{n2,m} = (-1 \mp k_{m+1} \mathbf{b}_{m+1} / k_m \mathbf{s}_m + k_{m+1} \mathbf{b}_{m+1} R_{m,m+1}) \exp(-\mathbf{b}_{m+1} l_{m+1}), \quad n = 1, 2; \quad (1g)$$

$$E_m = \frac{G_m}{\mathbf{b}_m^2 - \mathbf{s}_m^3}; \quad (1h)$$

$$G_m = \frac{\mathbf{b}_m I_0}{2k_m} \exp\left(-\sum_{i=m+1}^N \mathbf{b}_i l_i\right) \quad \text{for } m < N, \quad G_N = \frac{\mathbf{b}_N I_0}{2k_N}, \quad G_{N+1} = 0 \quad (1i)$$

In the equations above, $\mathbf{s}_i = (1 + j)a_i$, j is the complex constant $\sqrt{-1}$, $a_i = \sqrt{\rho f / \alpha_i}$ and l_i is the position of the interface between layer i and layer $i+1$. f is the modulation frequency, k_i is the thermal conductivity of layer i , $R_{i,i+1}$ is the contact resistance between layer i and layer $i+1$, and β_i is the optical absorption coefficient of layer i . It has been shown from generalized PA theory [3] that the amplitude of the PA signal can be calculated as:

$$A = abs\left[(1 - r) B_{N+1} P_0 / \sqrt{2} l_{N+1} a_{N+1} T_0\right] \quad (2)$$

where P_0 is the ambient pressure.

III. High Temperature Photoacoustic Apparatus

The schematic of the PA apparatus is shown in Fig.1. A fiber laser of wavelength $1.1 \mu\text{m}$ is modulated by an acoustic-optical modulator (AOM) whose frequency is controlled by a lock-in amplifier. The frequency used in this work varies from 1 kHz to 20 kHz. The laser beam is directed onto the sample which is mounted in the side wall the photoacoustic cell. The microphone senses the signal from the sample, and sends the signal to the preamplifier, conditioning amplifier and then the lock-in amplifier, which measures the acoustic signal at the modulation frequency. A PC is used to record data and control the experiments.

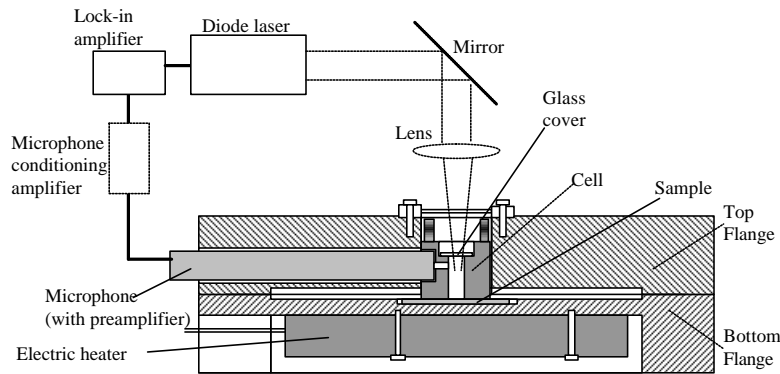


Figure 1. Schematic of the high temperature photo-acoustic apparatus.

The high temperature photoacoustic cell has a cylindrical geometry, which has a 4 mm inner diameter and 9.7 mm height. The cell is designed to be small enough to produce a strong

PA signal, but large enough so that a microphone can be inserted. The cell is made of sapphire, with a glass cover glued on the top. A spring is used to push the cell against the sample surface. The microphone (Model 4938 from Brüel & Kjær) with the preamplifier (Model 2670 from Brüel & Kjær) is inserted into the cell from an opening on the wall, and is sealed with Teflon tapes. The diameter of the microphone is 6.4 mm.

Sapphire is chosen to construct the cell for several reasons. The first is that it can be used at high temperatures. Also, it is transparent to the laser beam. Another cell made of steel was also tested. However, it was found that the steel cell did not work well due to multiple reflections of the scattered laser light within the cell. Absorption of light by steel also caused experimental error.

A top flange and a bottom flange are used to hold the sample, the microphone and the PA cell together. A glass window is mounted on the top flange to allow the laser beam to pass through. The top flange is fitted with a gas inlet (not shown in the figure). The use of the flanges and gas inlet allows the environment in the cell to be controlled. An electric heater is used to heat the sample. The temperatures of the heater and the sample surface are controlled by a thermostat.

The highest temperature that the sample can be measured at is limited by the maximum operation of the microphone and the preamplifier, which is 300 °C and 150 °C, respectively. Therefore, the highest temperature for the sample is about 150°C. By changing the thermal design of the cell, it is possible to lower the temperature of the pre-amplifier, therefore, to increase the temperature of the measurement. However, to our knowledge, there is no commercially available miniature microphone operated at temperatures higher than 300 °C.

A glass coated with 70 nm Ni is used as the reference. This reference and the sample are measured at two elevated temperatures (70°C and 110°C) as well as the room temperature. The theoretical signal of the reference sample $A_{ther,ref}$ is calculated from Equation 2. The experimentally measured amplitudes of the reference and the sample are denoted $A_{expr,ref}$ and $A_{expr,samp}$. The theoretical amplitude of the sample $A_{ther,samp}$ is therefore expressed as:

$$A_{ther,samp} = \frac{A_{exp r,samp}}{A_{exp r,ref}} A_{ther,ref} \quad (3)$$

Values of $A_{ther,samp}$ obtained at all the frequencies (from 1 kHz to 20 kHz) are then used in a least square fitting procedure to obtain the thermal conductivity of the sample.

IV. Experimental Results

In the experiment, both the sample and the reference are first measured using another PA cell constructed using acrylics. The acrylic cell has been shown to be able to provide accurate measurement of the thermal conductivity by comparing the measured data with the laser flash method and published data, with an accuracy of $\pm 5\%$ [7]. The sample used in this work is 1mm thick zirconium alloy with a 0.036 mm thick oxide layer on the surface. The thermal conductivity of the oxide is to be determined. Both the sample and the reference are coated with

70 nm Ni to obtain identical absorption of the laser energy. Knowing the absorption of the sample or having the same absorption for the reference and the sample is very important to obtaining accurate results.

The result of data processing is shown in Fig. 2. The value of the thermal conductivity of the sample (the oxide) at the room temperature is found to be $2.07 \text{ W/m}\cdot\text{K}$. The reference and the sample are then measured using the sapphire cell at the room temperature. The result is shown in Fig. 3, and the thermal conductivity is found to be $2.02 \text{ W/m}\cdot\text{K}$. This value is very close to the value obtained from the acrylic cell, indicating that the high temperature cell also provides accurate measurement results.

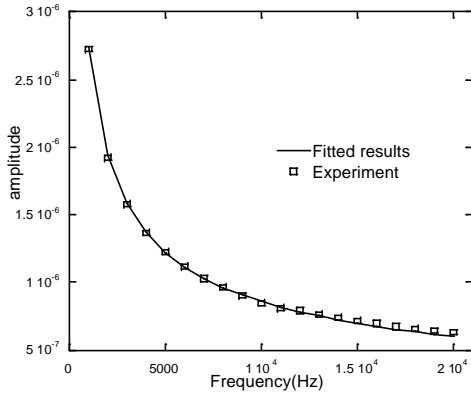


Figure 2. Amplitude of the photoacoustic signal and the fitting of thermal conductivity using the acrylic cell at the room temperature (24°C)

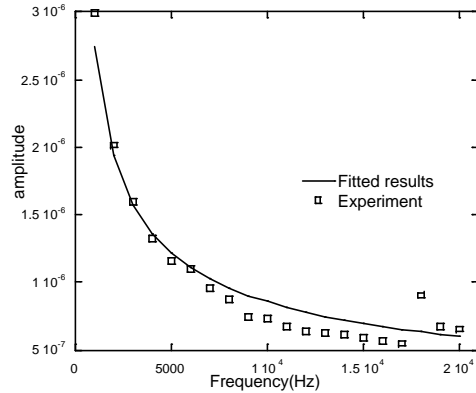


Figure 3. Amplitude of the photoacoustic signal and the fitting of thermal conductivity using the high temperature cell at the room temperature (24°C)

The reference and the sample are then measured at two elevated temperatures, 70°C and 110°C . The results are given in Fig. 4 and Fig. 5. The thermal conductivity obtained from the data processing is $2.21 \text{ W/m}\cdot\text{K}$ for 70°C and $2.24 \text{ W/m}\cdot\text{K}$ for 110°C . In the data processing, temperature dependent data of thermal conductivity, specific heat, and density of the alloy are used, while the specific heat and density of the oxide are room temperature data since the temperature dependent values are not available.

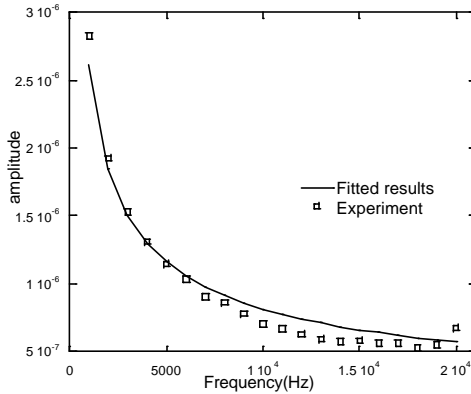


Figure 4. Amplitude of the photoacoustic signal and the fitting of thermal conductivity at the temperature of 70°C

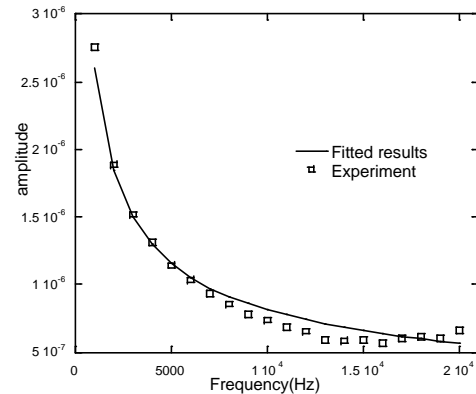


Figure 5. Amplitude of the photoacoustic signal and the fitting of thermal conductivity at the temperature of 110°C

The uncertainty of the PA signal amplitude is about 0.5%. It is shown from the uncertainty analysis that the thermal conductivity has an uncertainty of 0.1W/m•K [2].

It is seen from the experiment results that the thermal conductivity of the oxide slightly increases with the temperature increase. This trend of increase of thermal conductivity with temperature is in consistent with the general trend of the thermal conductivity of nonmetallic solids [1]. If the thermal design of the PA cell is optimized so that the measurement temperature can be increased, the dependence of thermal conductivity on temperature can be better evaluated.

V. Conclusions

This work presents using the photoacoustic (PA) technique to measure thermal conductivity at high temperatures. The design of a high temperature photoacoustic cell is described. The accuracy of the measurement apparatus is verified, and thermal conductivity of a ceramic sample at 70 °C and 110 °C is measured. Experiments at higher temperatures are possible if microphones operated at higher temperatures become available.

Reference:

1. F. P. Incropera and D. P. DeWitt, *Fundamentals of Heat and mass Transfer* (Wiley, New York, 2002).
2. X. Wang, H. Hu and X. Xu, J. Heat Transfer. **123**(1), 1 (2001).
3. H. Hu, X. Wang and X. Xu, J. Appl. Phys., **86**, 3953 (1999).
4. R. Rosencwaig and A. Gersho, J. Appl. Phys. **47**, 64 (1976).
5. F. A. McDonald and G. C. Wetsel, J. Appl. Phys. **49**, 2313 (1978).
6. K. D. Cole and W. A. McGahan, Micromechanical systems, Proceedings of winter annual meeting of the American Society of Mechanical Engineering (ASME, New York, 1992), p.267.
7. R. E. Taylor, X. Wang and X. Xu, Surface and Coating Technology, **120-121**, 89 (1999).